Signature inversion and the first observation of a magnetic dipole band in odd-odd rubidium isotopes: ^{82}Rb

J. Döring,[1,2] D. Ulrich,[1] G. D. Johns,[1,*] M. A. Riley,[1] and S. L. Tabor[1]
[1]*Department of Physics, Florida State University, Tallahassee, Florida 32306*
[2]*Department of Physics, University of Notre Dame, Notre Dame, Indiana 46556*
(Received 22 July 1998)

High-spin states in ^{82}Rb were studied through the ^{68}Zn(^{18}O,$p3n$) reaction at 56 MeV beam energy via a thin target coincidence measurement. The known sequence of positive-parity states built on the 6^+ state at 191.3 keV was extended up to spin 14, and signature inversion was observed around spin 11. Above spin 8 the observed properties of this band indicate a rotationlike structure. A new high-lying level sequence connected by $\Delta I=1$ transitions was identified. This magnetic dipole sequence is built on a new (11^-) level at 2617.3 keV excitation energy which is interpreted as a $\pi(g_{9/2})^2 \otimes \pi(p_{3/2},f_{5/2}) \otimes \nu g_{9/2}$ four-quasiparticle state at small quadrupole deformation. [S0556-2813(99)04301-0]

PACS number(s): 21.10.Re, 23.20.En, 23.20.Lv, 27.50.+e

I. INTRODUCTION

Collective high-spin bands built on low-lying isomers have been observed in a variety of neutron-deficient odd-odd nuclei in the mass 80 region, such as ^{74,76}Br [1–3] and ^{76,78}Rb [4,5], providing evidence for the occurrence of well-deformed nuclear shapes with a quadrupole deformation of $\beta_2 \approx 0.38$. However, the deformation depends strongly on the occupation of the proton and neutron intruder high-j $g_{9/2}$ subshells, in particular on the low-Ω orbitals. With increasing neutron number towards the neutron shell closure at $N=50$ this deformation-driving feature diminishes and the experimental excitation spectrum can be well explained in the framework of the spherical shell model, as recently demonstrated for the odd-odd nucleus ^{86}Rb [6].

For the nuclei in-between, the transitional character may be enhanced leading to a very fragile coexistence of excitation modes based on different deformations. Especially, in the odd-odd nuclei ^{84}Y [7] and ^{86}Nb [8] with 45 neutrons, the intruder $g_{9/2}$ subshell is half filled and has already lost most of its deformation driving capability. The competition of $g_{9/2}$ protons and $g_{9/2}$ neutrons in these nuclei yielded moderate deformations of $\beta_2 \approx 0.17$ for the rotationlike positive-parity high-spin band with the occurrence of signature inversion at spin 11. In addition to these $N=45$ nuclei, signature inversion was observed in the positive-parity yrast sequences of the lighter odd-odd ^{76,78,80}Rb isotopes [4,5,9,10] at spins 9 and 10. Thus, the present investigation was motivated by the question how this structural effect may be exhibited in the heavier but less-deformed $N=45$ odd-odd ^{82}Rb nucleus. Prior to the present work, there was no information available for states with $I>10$ in ^{82}Rb.

Further, in several odd-mass Br, Kr, Rb, and Y nuclei, fast $M1$ transitions [$B(M1) \approx 0.6$ Weisskopf units] between high-spin states have been identified [11,12], which are built on high-K three-quasiparticle states. In heavier nuclei with $A \approx 200$ observations of long $M1$ bands with only weak $E2$ crossover transitions [13] have been successfully interpreted using the concept of tilted rotation or the so-called ''Shears mechanism'' [14]. The fast $M1$ transitions are generated by a gradual alignment of the high-j proton and neutron angular momenta along the direction of the total spin. This effect is predicted to occur in weakly deformed nuclei throughout the chart of nuclides, including the mass 80 region [15]. Initial evidence has been found in odd-mass nuclei [11,12] and a search has been performed for an identification of such a $M1$ band in an odd-odd Rb nucleus.

Early spin and parity assignments of 1^+ to the ground state and 5^- to the long-lived isomeric state in odd-odd ^{82}Rb were based on a radioactive decay measurement [16]. Excited states in ^{82}Rb were investigated previously with the ^{81}Br(α,$3n$) reaction [17] where six transitions (and another tentatively) were assigned to a band structure in this nucleus. However, spins and excitation energies of the levels could not be given unambiguously since it was not clear at that time if the sequence was built on top of the 1^+ ground state or the long-lived 5^- isomer. This problem was solved in another experiment employing the ^{79}Br(α,n) and ^{78}Se(^{7}Li,$3n$) reactions [18,19] where the energy of the 5^- isomer was identified to be at 68.3 keV and the known decay sequence was found to feed into this isomer. Thus, states up to a (10^+) level at 1281 keV were observed, just below the expected spin range where signature inversion may take place. Therefore, a thin target coincidence experiment has been carried out using a heavy-ion reaction to populate high-spin states. Early results have been reported elsewhere [20].

II. EXPERIMENTAL TECHNIQUES

A thin target coincidence experiment was performed via the ^{68}Zn(^{18}O,$p3n$) reaction at 56 MeV beam energy. The ^{18}O beam was provided by the Florida State University Tandem–Superconducting LINAC facility and incident upon a 0.8 mg cm^{-2} self-supporting metallic Zn foil enriched to 99% in ^{68}Zn. The γ rays emitted during the bombardment were recorded with the Pittsburgh-Florida State Universities

*Present address: Los Alamos National Laboratory, Los Alamos, NM 87545.

detector array [21] consisting of 8 high-purity Ge detectors at the time. Each Ge detector had an efficiency of about 25% and was Compton-suppressed by shields made out of bismuth-germanate (BGO). Two detectors were placed at a forward angle of 35°, two detectors at 90°, and four detectors at 145°. Care was taken to adjust the electronic time window at about 100 ns to include somewhat coincidences with slow Ge-detector time signals usually generated by low-energy γ rays. Also, the thresholds in the fast timing electronics were set at about 40 keV for each Ge detector to accommodate for the known low-energy transitions at 45.6 and 64.2 keV of the positive-parity sequence. About 1.5×10^8 prompt events were stored on 8 mm tape. After energy calibration of each coincident event taking into account the Doppler shift of the γ rays, the events were sorted into a triangular matrix containing all prompt coincidence events (from 28 detector pairs), and into a square matrix where the events from the forward and backward detectors were sorted against the 90° detector events (12 detector pairs).

It should be mentioned that the $(^{18}O,p3n)^{82}Rb$ reaction channel is weak ($\approx8\%$) compared to the dominating pure neutron evaporation channels leading to $^{82,83}Sr$ isotopes which have about 22% and 37%, respectively, of the total yield. Also, the adjacent odd-mass nucleus ^{83}Rb [22] was produced to some extent ($\approx10\%$) via the $(^{18}O,p2n)$ reaction. The γ-ray energies, relative intensities, and spin and parity assignments of transitions assigned to ^{82}Rb are summarized in Table I.

To help in spin assignments the square coincidence matrix was analyzed with respect to directional correlation of oriented nuclei (DCO) ratios whenever possible for the transitions of interest. This ratio is given by

$$R_{\mathrm{DCO}}=\frac{I_{\gamma_1}(35°,145°)\ \text{gated by}\ \gamma_2\ \text{at}\ 90°}{I_{\gamma_1}(90°)\ \text{gated by}\ \gamma_2\ \text{at}\ 35°,145°}. \qquad (1)$$

The interpretation of the DCO ratios is most straightforward when gating is carried out on stretched $E2$ transitions. In this case DCO ratios of about 1.0 and 0.5 are expected for stretched $\Delta I=2$ and $\Delta I=1$ transitions, respectively. If dipole-quadrupole mixing is included, then the DCO ratio for a $\Delta I=1$ transition may vary between 0.2 and 1.8 depending on the amount of mixing and the nuclear alignment. Ambiguities may also occur since an unstretched pure $\Delta I=0$ transition is expected to have a ratio slightly larger than 1, i.e., similar to a stretched $E2$ transition [23,24].

The only $E2$ transition known in ^{82}Rb before the present work is the 980.4 keV $10^{(+)}\rightarrow8^{(+)}$ transition [17,18]. However, in using this transition, only a small fraction of the new lines assigned to ^{82}Rb can be analyzed. Therefore, we also used the low-lying 123.0 keV $6^+\rightarrow5^-$ transition which has an $E1$ character [18] as a gate. The thresholds in the Ge detector coincidence circuit were set low enough and the time window wide enough to have a very good coincidence efficiency at this energy. The DCO ratio for the 123.0 keV γ ray in the 980.4 keV $E2$ gate is close to 0.5, as expected for a stretched dipole transition, and a $M2$ admixture seems to be very unlikely based on the measured lifetime of the 6^+ level [18,25]. Therefore, this transition was used as gate for other transitions in coincidence. A renormalization of the DCO ratios obtained from the 123 keV gate by a factor of 0.5 was applied as necessary for comparison with DCO ratios deduced from $E2$ gates. Furthermore, DCO gates were set on other $\Delta I=1$ transitions such as the 207 and 416 keV as well as the 411 and 473 keV transitions. Individual DCO ratios are given in Table I together with the gating conditions.

III. LEVEL SCHEME OF ^{82}Rb AND SPIN-PARITY ASSIGNMENTS

A. Positive-parity yrast sequence

The new ^{82}Rb level scheme as deduced from our experiment is shown in Fig. 1. The known [18] band of positive parity built on the low-lying 6^+ level at 191.3 keV has been extended up to a $14^{(+)}$ state at 4015.9 keV. Two coincidence gates, set on the 563 and the 980 keV transitions, are displayed in Fig. 2. The highest observed transition is a 1464.2 keV γ ray depopulating the spin 14 state. DCO ratios have been determined for the $\Delta I=1$ and 2 transitions up to spin 14 leading to firm spin assignments. There is good agreement between the ratios determined from the 980 keV $E2$ gate and the renormalized ratios deduced from the 123 keV $E1$ gate. The small ratio for the 64.2 keV $\Delta I=1$ transition may be caused by different Ge detector efficiencies at this low γ-ray energy rather than dipole-quadrupole mixing.

The yrast nature of the states and the strong $\Delta I=2$ intraband transitions provide evidence that both decay sequences are signature partners, despite the detection of only two (three) $\Delta I=2$ transitions in the odd-spin (even-spin) decay sequence above the $8^{(+)}$ state. Further, an interesting feature of this yrast band is that intense interconnecting $\Delta I=1$ transitions such as the 562.6, 620.9, and 632.0 keV transitions have been observed only in one direction, from odd-spin to even-spin states. For the other way around, the $\Delta I=1$ transitions are weak or missing. Thus, for the $12^{(+)}\rightarrow11^{(+)}$649.5 keV transition, an upper intensity limit could be estimated only from the 123 keV gate (see Table I). However, this particular decay feature provides additional evidence for the bands being signature partners (see Sec. IV A).

Positive parity for the 6^+ bandhead state was inferred previously from angular distribution and polarization measurements [18]. It is supported by the recently measured g factor [25]. For the states above it positive parity is tentatively given only due to the uncertainties with the 45.6 and 64.2 keV transitions. Both transitions have a $\Delta I=1$ character based on the measured angular distribution coefficients [18]. An almost pure multipolarity of $M1$ is expected because of the low transition energies and their observation in prompt coincidences. However, an $E1$ nature cannot be completely ruled out. The fact that the states in this band are yrast further supports the $M1$ nature of the 45.6 and 64.2 keV transitions and thus positive parity for the states since the yrast bands in most odd-odd nuclei in this mass region have positive parity.

A transition at 839.5 keV was observed in coincidence with the 562.6 keV line establishing a level at 1703.2 keV. This sidefeeding transition is not a part of the rotationlike yrast sequence and may demonstrate shell-model influence.

TABLE I. Experimental results for states in ^{82}Rb.

E_{level} [a] (keV)	I_i^π [b]	I_f^π [c]	E_γ [d] (keV)	I_γ [e]	R_{DCO} [f]	$E2$ gate [g] (keV)	R_{DCO} [h]	$\Delta I=1$ gate [g] (keV)	σL [i]
191.3	6^+	5^-	123.0(1)	100(2)	0.50(3)	980	0.48(5)	411+473	$E1$
209.2		6^+	17.8(2) [j]						
255.5	$7^{(+)}$	6^+	64.2(1)	65(4)	0.22(6)	980	0.34(3)	123	$(M1)$
301.1	$8^{(+)}$	$7^{(+)}$	45.6(2)	55(12)					$(M1)$
393.5	$(6^-,7^-)$	5^-	325.2(1)	20(2)	0.97(16)	963	1.08(15)	411+473	$(E2)$
484.0	6^-	5^-	415.7(1)	27(3)			0.51(4)	207	$M1/E2$
538.5	(6)	$7^{(+)}$	283.0(2)	3(1)			0.81(19)	123	
575.4	(5)	6^+	383.9(2)	≈ 1					
690.6	7^-	6^-	206.6(1)	21(2)			0.58(5)	416	$M1/E2$
							0.65(7)	411+473	
		(7^-)	296.8(3)	3(1)	1.05(12)	325			$(M1/E2)$
		$7^{(+)}$	435.2(3)	2(1)					$(E1)$
		6^+	499.2(3)	2(1)			0.58(15)	123	$E1$
		5^-	622.5(3)	≈ 1					$(E2)$
704.5	(6)	(5)	129.0(3)	≈ 1					
			495.1(3)	2(1)					
734.0	(7)	$8^{(+)}$	433.1(3)	2(1)					
		6^+	542.6(2)	3(1)					
771.0		(6)	233.3(3)	≈ 1					
863.7	$9^{(+)}$	$8^{(+)}$	562.6(1)	25(2)			0.56(4)	123	$M1$
898.9	(7)	(6)	194.4(3)	2(1)					
		6^+	707.5(3)	3(1)					
1024.9	(8^+)	(7)	125.9(3)	3(1)					
		6^+	833.6(3)	7(1)			1.04(16)	123	$(E2)$
1084.4	7^-	7^-	393.8(2)	5(1)			0.91(8)	207+416	$M1/E2$
		6^-	600.9(5)	4(1)			0.53(10)	416	$M1/E2$
1210.8	(9^+)	(8^+)	186.0(2)	2(1)			0.81(13)	123	$(M1/E2)$
		$7^{(+)}$	955.3(3)	6(1)			0.87(15)	123	$(E2)$
1281.5	$10^{(+)}$	$9^{(+)}$	417.7(2)	4(1)			0.63(8)	123	$M1$
		$8^{(+)}$	980.4(1)	31(2)			1.12(8)	123	$E2$
1356.5	$(8^-,9^-)$	7^-	666(1)	≈ 1					
		$(6^-,7^-)$	963.0(2)	18(2)	1.12(11)	325			$E2$
		$8^{(+)}$	1055.2(5)	2(1)					$(E1)$
1703.2	$10^{(+)}$	$9^{(+)}$	839.5(2)	10(1)			0.45(12)	123	$M1/E2$
1732.4	(9^-)	7^-	1041.8(4)	13(2)			0.78(11)	207+416	$(E2)$
1844.1	(9^-)	7^-	759.7(3)	7(1)			0.82(15)	207+416	$(E2)$
		$8^{(+)}$	1543(1)	2(1)					$(E1)$
1902.4	$11^{(+)}$	$10^{(+)}$	620.9(2)	12(1)	0.54(4)	980	0.52(7)	123	$M1/E2$
		$9^{(+)}$	1038.4(3)	5(1)			0.98(16)	123	$E2$
1962.7	$10^{(+)}$	$9^{(+)}$	1099.0(2)	4(1)			0.43(10)	123	$(M1/E2)$
2290.9	$11^{(+)}$	$10^{(+)}$	587.7(3)	3(1)			0.56(13)	123	$M1/E2$
2395.1	$(10^-,11^-)$	$(8^-,9^-)$	1038.6(4)	16(2)	1.09(11)	325			$E2$
2551.7	$12^{(+)}$	$11^{(+)}$	261.1(3)	≈ 1					$(M1)$
		$11^{(+)}$	649.5(4)	<1					$(M1)$
		$10^{(+)}$	1270.2(3)	12(2)	0.95(7)	980	0.97(13)	123	$E2$
2617.3	(11^-)	$(10^-,11^-)$	222.4(2)	6(1)	0.94(12)	325	0.69(8)	411+473	$(M1/E2)$
		(9^-)	773.0(3)	6(1)			1.15(19)	411+473	$(E2)$
		(9^-)	885.1(3)	3(1)					$(E2)$
		$10^{(+)}$	913.9(3)	3(1)			0.50(14)	123	$(E1)$
2709.7	(11^-)	(9^-)	977.1(3)	4(1)					$(E2)$
3027.9	(12^-)	(11^-)	318.0(3)	≈ 1					$(M1)$
		(11^-)	410.6(2)	14(2)	0.60(10)	325	0.53(8)	123	$M1$
3183.8	$13^{(+)}$	$12^{(+)}$	632.0(3)	4(1)			0.49(12)	123	$M1/E2$
		$11^{(+)}$	1281.4(4)	5(1)			0.93(19)	123	$E2$
3501.0	(13^-)	(12^-)	473.1(2)	11(2)			0.49(10)	123	$M1$
							0.44(6)	207+416	
4015.9	$14^{(+)}$	$12^{(+)}$	1464.2(5)	6(1)			1.1(2)	123	$E2$
4048.7	(14^-)	(13^-)	547.7(3)	8(2)			0.56(8)	411+473	$M1$
							0.44(8)	207+416	
4717.2	(15^-)	(14^-)	668.5(4)	3(1)					$(M1)$

[a] Level energy.

[b] Spin and parity of the initial state.

[c] Spin and parity of the final state.

[d] Transition energy. Uncertainty is given in units of the last decimal.

[e] Relative γ-ray intensity determined from the triangular matrix.

[f] DCO ratio as deduced from the $E2$ gate given in next column.

[g] Gate energy used to determine the DCO ratio.

[h] Renormalized (divided by 2.0) DCO ratio as deduced from the $\Delta I=1$ gate.

[i] Multipolarity of the transition.

[j] Observed in data set of Ref. [18].

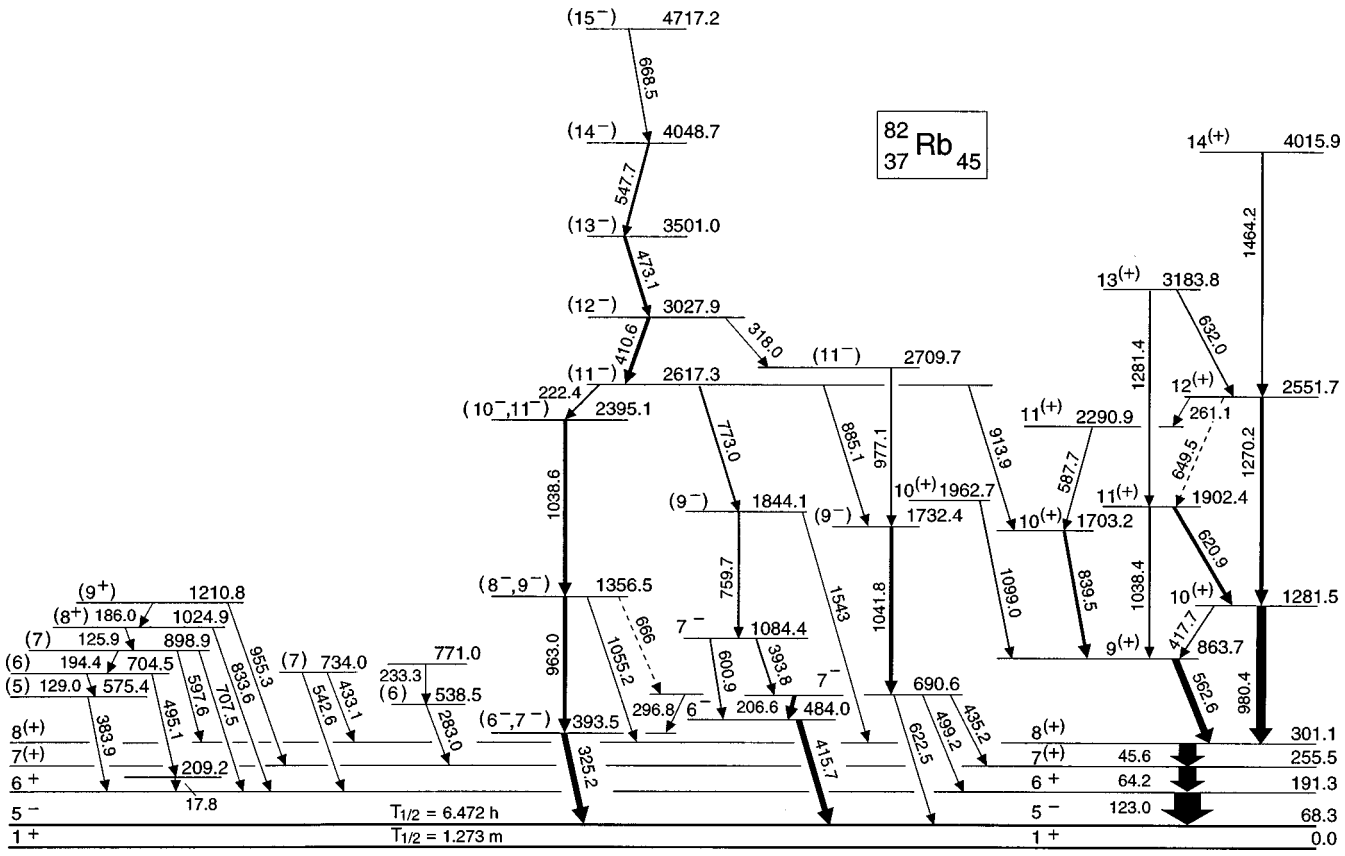

FIG. 1. Level scheme of odd-odd ^{82}Rb as deduced from the present experiment. Spin and parity assignments of 1^+ and 5^- for the ground state and the long-lived isomer, respectively, as well as assignments for some low-lying states, have been taken from Refs. [16,18].

The 1703.2 keV level is fed by two weak transitions at 587.7 keV and 913.9 keV. The latter one provides a link to a new high-spin dipole sequence.

B. High-lying magnetic dipole band

This structure is unique for ^{82}Rb and has not been seen in another odd-odd Rb isotope. The band is built on the level at 2617.3 keV. The coincidence relationships of transitions involved in this new $\Delta I=1$ high-spin level sequence can be seen in Fig. 3 where three samples of background-subtracted coincidence spectra are shown. Two gates, the 325 and 416 keV lines, represent low-lying transitions fed through the depopulation of the high-lying band, whereas the 473 keV γ ray is a member of the $\Delta I=1$ sequence.

The new band shows the following features: (i) The decay out of the lowest level at 2617.3 keV proceeds through several transitions to positive- and negative-parity states. No decay preference is observed based on the relative intensities of the transitions involved. (ii) The band contains four

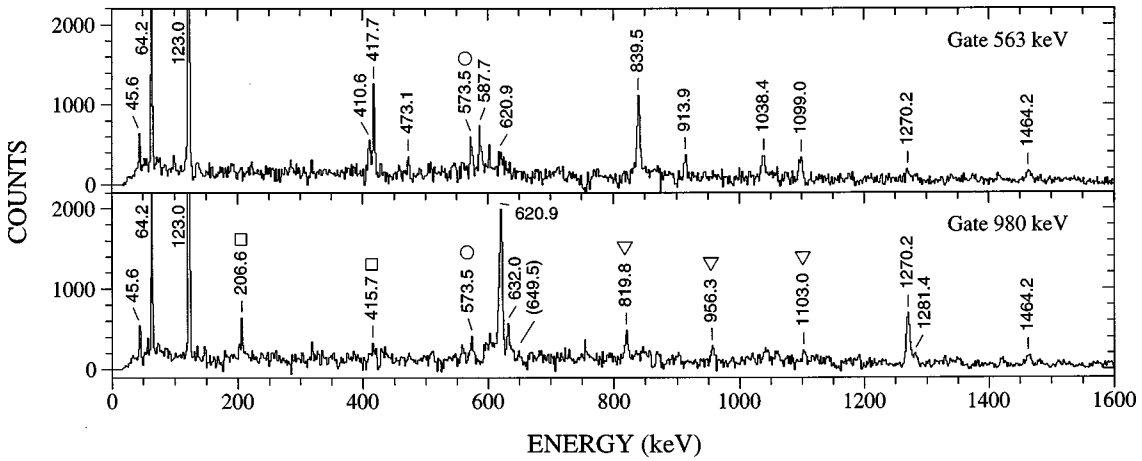

FIG. 2. Samples of background-corrected coincidence spectra relevant for the extension of the positive-parity level sequence. The transitions assigned to ^{82}Rb are marked with their energy in keV. Open symbols are used to indicate contaminations from known transitions: square, 977 keV in ^{82}Rb; triangle, ^{80}Kr; circle, ^{82}Sr.

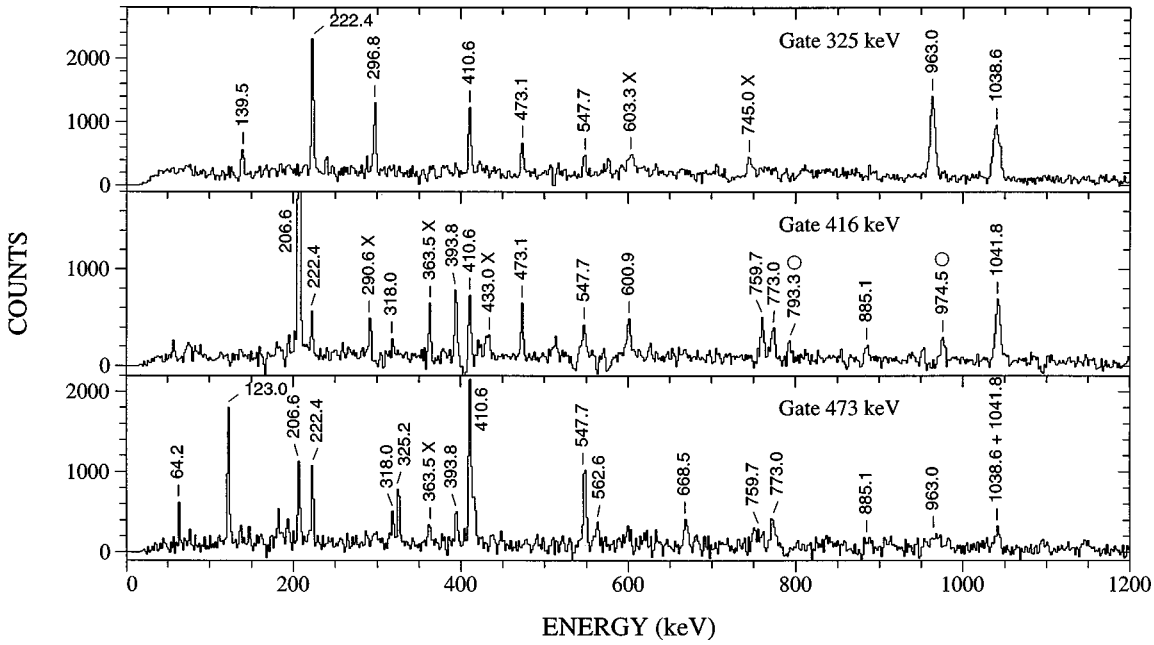

FIG. 3. Samples of background-corrected coincidence spectra relevant for the high-lying $\Delta I=1$ sequence. All transitions assigned to ^{82}Rb are labeled with their energy in keV. Contaminant transitions from ^{84}Sr are labeled with open circles and lines not assigned are marked with the letter X.

$\Delta I=1$ transitions. (iii) No crossover transitions between $\Delta I=2$ states of the band were observed within our statistical limits.

The DCO ratios for the 410.6, 473.1, and 547.7 keV transitions clearly indicate a $\Delta I=1$ character. To deduce these ratios, gates were set on several low-lying $\Delta I=1$ and 2 transitions. The ratios extracted from the established 123 keV gate contain large errors; therefore, another depopulation path via the $\Delta I=1$ transitions at 206.6 and 415.7 keV has been used as well. Both transitions were assumed to be almost pure $M1$ in character based on the angular distribution coefficient measured in Ref. [18]. In this case a small $E2$ component does not affect the deduced DCO ratios much. Therefore, the added (207 + 416 keV) spectra were analyzed with regard to the higher-lying transitions. The results were renormalized by a factor of 0.5 for comparison with $E2$ gated DCO ratios. In this way, consistent results emerged for the high-lying transitions supporting the $\Delta I=1$ nature. The uppermost 668.5 keV transition is too weak and too close in energy to a tentatively placed low-lying linking transition. Therefore, no reliable DCO ratio could be extracted for it.

Further, the gates set on the 411 and 473 keV transitions of the high-lying $M1$ band have been added and analyzed as well to deduce DCO ratios, in particular for the low-energy lines at 206.6 and 222.4 keV. The gated spectra from which these DCO ratios were determined are shown in Fig. 4. Individual results for a few lines are given in Table I too. The intensity pattern of the 206.6 and 222.4 keV lines is very similar in these spectra which are gated by transitions above both lines. Thus, it is likely that the 222.4 keV line has a $\Delta I=1$ character too. It should be noted that the measured DCO ratios for the 773.0 and 759.7 keV decay sequence depopulating the 2617.3 keV level are compatible with an $E2$ nature of these transitions. However, no DCO value could be extracted for the 885.1 keV transition due to limited statistics.

A spin 11 assignment to the 2617.3 keV level seems to be the best choice; however, it leads to a contradiction with the spin and parity assignments of 5^+ made previously [18] to the level at 393.5 keV. This level is populated via the decay branch containing the 963.0, 1038.6, and 222.4 keV transitions from the 2617.3 keV level. The coincidence relations are certain and the energies match up quite well. The 393.5 keV level decays further by a 325.2 keV directly to the isomeric 5^- state. In case of the previously made 5^+ assignment a spin difference of 6 would have to be carried away by three transitions, including a parity change. However, a $M2$ assignment to one of the transitions can be excluded due to their observation in the prompt coincidence measurement. For example, the assumption of a $M2$ character for the 325.2 keV transition would imply a level lifetime of at least 630 ns

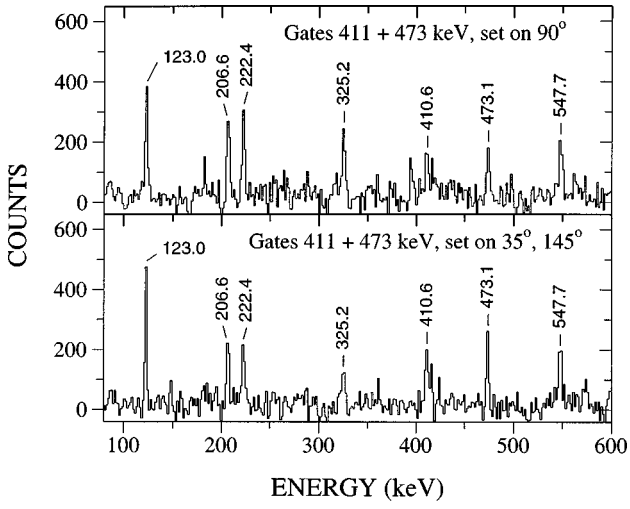

FIG. 4. Background-corrected sum spectra used to extract DCO ratios for several transitions. The 411 and 473 keV gating transitions are members of the new high-lying magnetic dipole band.

to obtain a $M2$ transition probability below the recommended upper limit of 1 Weisskopf unit [26].

The positive A_2 angular distribution coefficient measured previously [18] and the present average DCO ratio of 1.02 for the 325.2 keV line can also be understood when a spin and parity of 7^- are assumed for the 393.5 keV level. This would lead to an $E2$ nature of the 325.2 keV transition. However, the measured linear polarization [18] would be in disagreement. Further, a 6^- assignment might be possible for the 393.5 keV level since strong dipole-quadrupole mixing ($\delta \approx +2.3$) of the 325.2 keV transition can account for the observed DCO ratio and the previously measured angular distribution coefficients. The 6^- possibility does not, however, remove the disagreement with the previously measured polarization. A weak line at 296.8 keV has been seen in coincidence with the 325.2 keV transition which provides a link to the known 7^- level at 690.6 keV. Since $M2$ decay is extremely unlikely for the 296.8 keV transition, its occurrence contradicts the earlier 5^+ assignment to the 393.5 keV level. The likely $M1/E2$ character of the 296.8 keV line is consistent with both possible spin-parity assignments of 6^- and 7^- discussed above.

In conclusion, both spins are possible from the current data, with the 6^- assignment somewhat favored. Further, the strong population of the 393.5 keV level in the (α,n) reaction [18] supports the lower spin assignment with a strongly mixed 325.2 keV decay to the 5^- isomer. However, due to these assignment problems, both spin possibilities are given for the sequence feeding into the 393.5 keV level. Also, all spins for the high-lying $M1$ band are given in parentheses.

C. Additional states feeding into the 5^- isomer

There are additional weakly populated levels which decay mainly to the low-lying 6^+,$7^{(+)}$, and $8^{(+)}$ states, e.g., via transitions at 383.9, 495.1, 597.6, 707.5, 833.6, and 955.3 keV (see left-hand side of Fig. 1). This new side structure is not connected to the other high-spin sequences. The low-energy connecting transitions are weak in intensity. The level at 704.5 keV excitation energy decays via the 129.0 and 495.1 keV transitions. The observed coincidence of the 495.1 keV transition with the 123.0 keV line points to the presence of a low-energy 18 keV transition not seen in this experiment. However, an inspection of the unpublished Leps-Ge(Li) coincidence data set of Ref. [18] measured via the (α,n) reaction shows, e.g., low-energy lines at 17.8 and 20.4 keV in coincidence with the 123.0 keV transition. The 17.8 keV transition fits the energy difference quite well, and thus a level at 209.2 keV is introduced. The proposed spin assignments for the side levels are partly based on DCO ratios deduced from the 123 keV gate. Additional weak transitions at 132.5, 344.8, 892.2, and 1346 keV have been seen in coincidence with the 123.0 keV transition but not placed into the level scheme.

IV. DISCUSSION

A. Systematics of signature inversion in odd-odd Rb isotopes

The extension of the high-spin positive-parity sequence in ^{82}Rb provides evidence for signature inversion around spin 11. The normalized energy difference of the states, also called the moment-of-inertia parameter within the rotational model, is shown in Fig. 5. For comparison, also the known data for ^{76,78,80}Rb are plotted. In all four nuclei, a zig-zag pattern is inferred, with a phase change at spin 11 in ^{82}Rb. This happens at the same spin as in the heavier $N=45$ odd-odd nuclei ^{84}Y and ^{86}Nb. A similar phase change or signature inversion is seen experimentally in most of the lighter odd-odd Rb isotopes but at lower spins, e.g., at spin 9 in ^{76,78}Rb and spin 10 in ^{80}Rb. The signature inversion observed in odd-odd ^{82}Y [27] takes place again at spin 9.

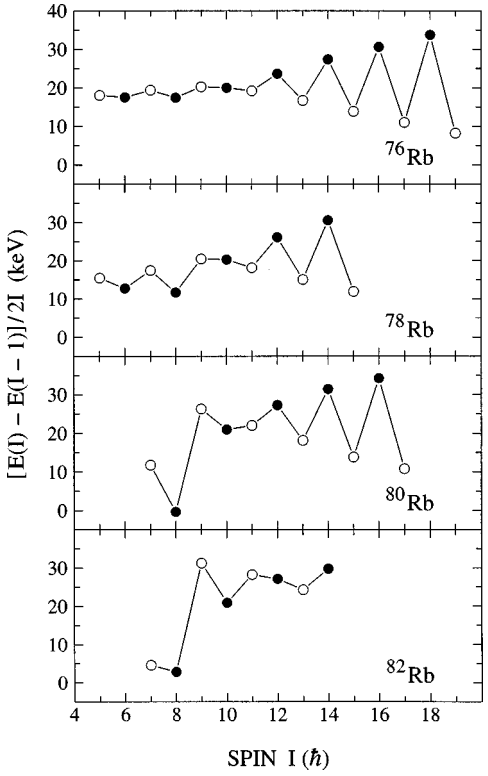

FIG. 5. Normalized energy difference for the positive-parity sequences in ^{82}Rb and lighter odd-odd Rb isotopes as a function of the spin of the initial state. Full (open) circles represent even-spin (odd-spin) values. The experimental data were taken from ^{76}Rb, Ref. [4]; ^{78}Rb, Ref. [5]; ^{80}Rb, Refs. [9,10].

Different explanations for signature inversion have been offered, mainly for nuclei in the mass 150 region. This includes the responsibility of high-j intruder orbitals [28] and their respective filling, shape fluctuations [29], the influence of the proton-neutron interaction [30], and Coriolis mixing within an axially symmetric rotor plus two-particle model [31]. The effect has also been seen in the $A \approx 120$ mass region, i.e., in the $\pi h_{11/2} \otimes \nu h_{11/2}$ bands [32–34]. It has been pointed out [35] earlier that the signature inversion in the mass 80 region is related to the filling of the high-j $g_{9/2}$ proton and $g_{9/2}$ neutron subshells and reflects the transition from mainly single-particle excitations at low spins to more rotational (collective) motion at higher spins. In the odd-odd Rb chain, the shift from spin 9 to 11 seems to be correlated with the nuclear quadrupole deformation, which decreases from ^{76,78}Rb ($\beta_2 \approx 0.38$) towards ^{82}Rb ($\beta_2 \approx 0.2$). But within the $N=45$ chain, ^{82}Rb, ^{84}Y, and ^{86}Nb, the signature inversion remains at spin 11 indicating only moderate deformation changes.

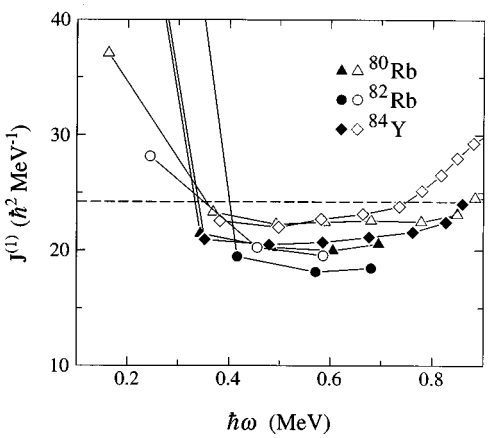

FIG. 6. Kinematic moments of inertia for the positive-parity bands in ^{82}Rb, ^{80}Rb [9,10], and ^{84}Y [7]. Solid (open) symbols represent signature $\alpha=0$ even-spin sequence ($\alpha=1$ odd-spin sequence). A value of $K=6$ has been used in the analysis. The horizontal dashed line represents the moment of inertia for a rigid rotation of an oblate nucleus with $A=82$ and $|\beta_2|=0.20$.

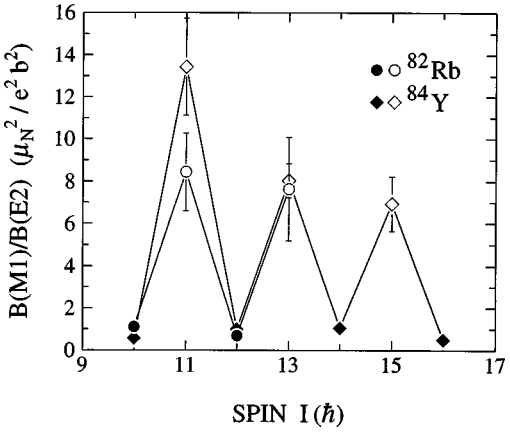

FIG. 7. Ratio of $M1$ to $E2$ transition strengths deduced from $\Delta I=1$ and 2 transitions in the positive-parity bands of ^{82}Rb and ^{84}Y [7] as a function of the spin of the initial state. Points corresponding to even-spin (odd-spin) states are shown with full (open) symbols.

The regular increase in energy spacing of the yrast positive-parity band above spin 8 in ^{82}Rb and its similarity with other bands in nearby odd-odd nuclei points to a rotationlike character. To probe this similarity, the kinematic moments of inertia of the yrast bands in ^{82}Rb, adjacent ^{80}Rb [9,10], and ^{84}Y [7] were deduced from the experimental energies and spins using the standard cranked-shell model formalism [36] and are plotted as a function of the rotational frequency in Fig. 6. After the irregularities at low spins the kinematic moments of inertia stay almost constant and somewhat below the rigid-body value in the frequency range of 0.4 to 0.7 MeV. At higher frequencies an increase occurs in the ^{80}Rb and ^{84}Y values which has been associated with quasiparticle alignment. The moment of inertia for a rigidly rotating oblate-deformed nucleus with $A=82$ and $|\beta_2|=0.20$ is shown as a dashed line in Fig. 6. It is given in first order of β_2 according to Ref. [37] by $J_{ri}=(2/5)AmR_0^2[1-(5/4\pi)^{1/2}\beta_2\cos(120°+\gamma)]$ where A is the mass number, m is the average nucleon mass, $R_0=r_0A^{1/3}$ is the nuclear radius with $r_0=1.2$ fm, and γ represents the triaxiality parameter which is here $0°(+60°)$ for a prolate (oblate) shape. In general, the rigid-body moment of inertia does not vary much with deformation, e.g., for a nucleus with $A=82$ from 21.5 $\hbar^2$/MeV at a spherical shape to 28.3 $\hbar^2$/MeV for an oblate-deformed nucleus with $|\beta_2|=0.5$. In the frequency range of 0.4 to 0.7 MeV, the ^{82}Rb values for the moment of inertia are about 15% lower when compared to ^{80}Rb and ^{84}Y which may be caused by a lower deformation of ^{82}Rb. However, the relatively constant values of $J^{(1)}$ suggest an onset of collective rotational behavior above states with spin 8.

Besides the moments of inertia, strong alterations of $B(M1)/B(E2)$ ratios have been found to be a typical feature of signature-partner sequences in the positive-parity yrast states of odd-odd nuclei in the mass 80 region [27]. This is of particular interest for bands where no level lifetime information is available. The ratio involves the $M1$ transition strengths between signature partners and the intraband $E2$ strengths and can be deduced directly from the transition energies and γ-ray intensities, e.g., see [38]. Experimental values are shown in Fig. 7 for the bands in ^{82}Rb and ^{84}Y. In extracting these values, a possible but small dipole-quadrupole mixing for the $\Delta I=1$ transitions has been neglected which is supported by the measured DCO ratios. In any case, a small quadrupole contribution does not change the ratio much.

Large alterations occur in the $B(M1)/B(E2)$ ratio, and the band in ^{82}Rb behaves very similarly to previous observations for yrast positive-parity bands in adjacent odd-odd nuclei, such as ^{78}Rb [5], ^{82}Y [27], ^{84}Y [7], and ^{86}Nb [8]. To illustrate this similarity, the ^{84}Y values are shown in Fig. 7 for comparison since the positive-parity band in ^{84}Y is known to much higher-spin states and its collectivity has been probed by lifetime measurements. The amplitudes may vary from nucleus to nucleus, but they always occur with the same phase, i.e., the $M1$ transition from the even-spin to the odd-spin state is much weaker than vice versa. Since in a collective structure the intraband $E2$ transition strengths usually vary smoothly with spin, the alterations can be associated with the variations in the $M1$ strengths, as demonstrated by two-quasiparticle plus triaxial rotor calculations for odd-odd ^{84,82}Y [7,27]. In this model the $M1$ transitions from an odd-spin state to the lower even-spin state are strong because they involve a change in the quasiparticle-core coupling only, while those from even-spin to odd-spin states are much weaker because they involve changes in the rotational states of the core. A possible triaxiality of the nuclear shape does not change the phase in the $B(M1)/B(E2)$ ratios but rather the amplitude which is sensitive to the contributions from the odd proton and the odd neutron to the total $M1$ strengths. Thus, the weak $12^{(+)}\rightarrow 11^{(+)}$ 649.5 keV transition between signature-partner states can be understood well in terms of the established systematics. However, the weak 261.1 keV transition from the same level to another higher-lying 11^+ state indicates that the 12^+ state is not a pure rotational state and may have four-quasiparticle (qp) contributions in its wave function.

B. Hartree-Fock-Bogoliubov shape calculations for ^{82}Rb

Shape calculations using the Hartree-Fock-Bogoliubov formalism [39] were carried out for positive- and negative-

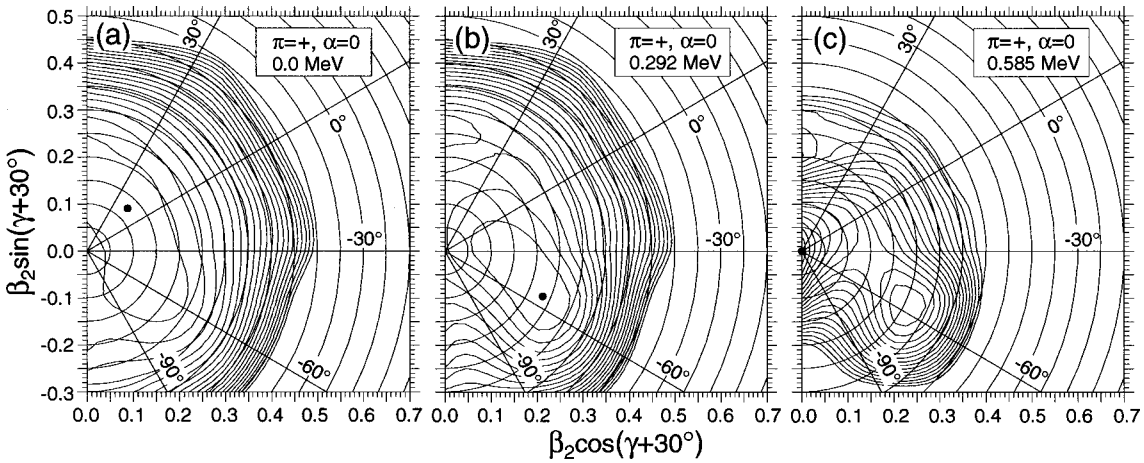

FIG. 8. TRS plots in the (β_2,γ) polar coordinate system for the positive-parity states in ^{82}Rb with signature $\alpha=0$. The rotational frequency is given in the inset. A prolate (oblate) shape corresponds to a triaxiality of $\gamma=0°(-60°)$. The contour lines are separated by 200 keV.

parity states in ^{82}Rb. A Woods-Saxon potential was used to describe the single-particle motion. A short-range monopole pairing force was included, and the cranking approximation was utilized to describe the rotation. Samples of total Routhian surfaces (TRS) for ^{82}Rb are presented in Fig. 8 in the polar coordinate plane (β_2,γ) for positive-parity states and in Fig. 9 for negative-parity states. At each grid point, the total Routhian was minimized with respect to the hexadecapole deformation β_4. The labeling scheme of Ref. [40] was used, where lower (upper) case letters are used for the proton (neutron) configuration. Thus, the lowest two-quasiparticle proton-neutron configuration in Fig. 8 is labeled bA [b: proton in configuration (parity, signature) $=(+,-1/2)$; A: neutron in configuration $(+,+1/2)$] yielding an overall positive parity and signature $\alpha=0$. Likewise, the lowest 2qp proton-neutron configuration of negative parity and signature $\alpha=1$ as shown in Fig. 9 corresponds to the configuration fA [f: proton in $(-,+1/2)$; A: neutron in $(+,+1/2)$].

For positive-parity states at low rotational frequency, i.e., configuration bA at $\hbar\omega\leqslant 0.292$ MeV, the calculations predict that the nucleus ^{82}Rb is very γ soft with a quadrupole deformation of at most $\beta_2\approx 0.23$, as can be seen in Fig. 8. With increasing frequency, the nucleus becomes slightly more deformed and more stiff at an oblate shape ($\beta_2\approx 0.25$, $\gamma=-57°$). The same pattern was calculated for the signature partner configuration aA with $\alpha=1$ (not shown).

For negative-parity states at low rotational frequency, the TRS calculations predict an almost spherical shape for such configurations where the valence neutron is occupying the $g_{9/2}$ subshell, e.g., for the fA and eA configurations. This is no surprise since for 45 neutrons the $g_{9/2}$ subshell is half filled and the deformation driving property of the neutron configuration is strongly reduced. At a higher frequency, e.g., at 0.487 MeV, two minima develop at a less-deformed near-prolate and a near-oblate shape. However, the near-oblate minimum disappears again with further increasing frequency.

The TRS calculations for the negative-parity states where the valence proton occupies the $g_{9/2}$ subshell predict a somewhat different shape for ^{82}Rb. At low rotational frequency, the shape is calculated to be weakly deformed ($\beta_2\leqslant 0.20$) with a quite large γ softness. At higher frequencies, the

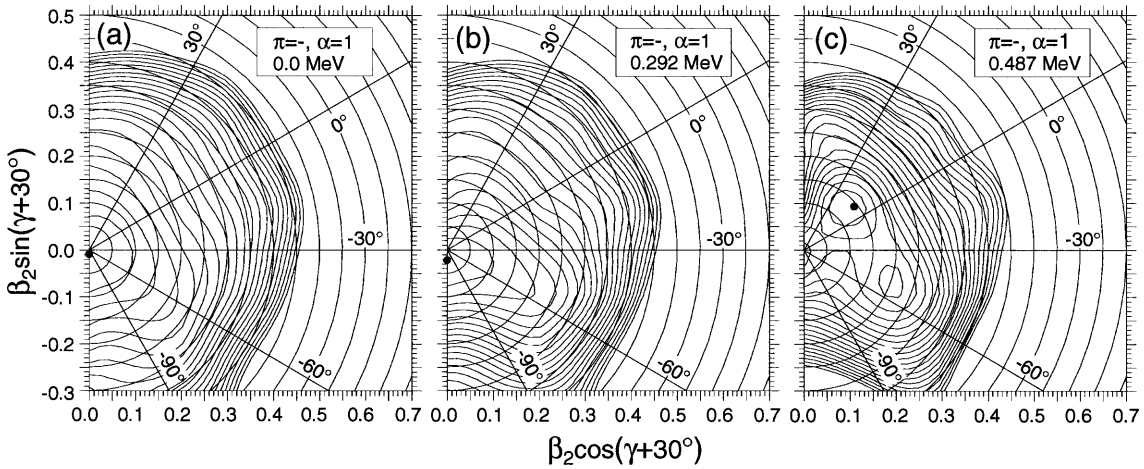

FIG. 9. TRS plots in the (β_2,γ) polar coordinate system for the negative-parity states in ^{82}Rb with signature $\alpha=1$. See caption of Fig. 8 for more details.

shape becomes more stiff at smaller deformation ($\beta_2 \leqslant 0.10$). In general, the TRS calculations support the conclusion that the ^{82}Rb nucleus does not have a stable deformation at low spins.

C. Low-lying negative-parity states

The low-lying negative-parity states in ^{82}Rb do not show the rotational behavior known from its neutron-deficient odd-odd Rb neighbors. This indicates a substantially smaller quadrupole deformation and clearly exhibits the transitional nature of this nucleus. This nature is also reflected in the magnetic moment for the 5^- isomeric state [41,42] in ^{82}Rb which can be explained quite well on the basis of spherical shell-model considerations by coupling a $p_{3/2}$ proton to the unusual neutron $(g_{9/2})^3_{7/2}$ configuration. A similar situation was found for the magnetic moment of the 5^- isomer in the lighter $N=45$ nucleus ^{80}Br [43,44]. Recently, also the measured magnetic moment of the 6^+ state at 191.3 keV in ^{82}Rb has been interpreted containing the same seniority-3 $g_{9/2}$ neutron configuration coupled to a $g_{9/2}$ proton [25].

An attempt has been made to apply qualitative shell-model considerations to the negative-parity states in ^{82}Rb. As already pointed out [18], the low-lying 6^- and 7^- states at 484.0 and 690.6 keV, which are separated by only 207 keV, are very likely based on the 2qp configurations $(\pi p_{3/2} \otimes \nu g_{9/2})_{6^-}$ and $(\pi f_{5/2} \otimes \nu g_{9/2})_{7^-}$, respectively. This proposal is based on the assumption that the unpaired neutron occupies the $g_{9/2}$ subshell which is the case at very small deformation. A spin of 7 is the highest possible spin which can be obtained within the spherical shell model for two-particle excitations of negative parity. Higher-spin states have to be connected with the creation of additional unpaired quasiparticles which costs quite a lot of energy. Only in case of a finite deformation the unpaired proton may occupy the $g_{9/2}$ subshell at low excitation energies as well, and a greater variety of low-lying states is expected for positive- and negative-parity states. In the framework of the spherical shell model, such proton excitations are estimated to be at much higher energies. The occurrence of positive-parity states of the $\pi g_{9/2} \otimes \nu g_{9/2}$ configuration at low energies points to the presence of these $g_{9/2}$ proton excitations. The consequences for negative-parity states are, however, difficult to assess due to the limited experimental information.

D. High-lying $M1$ band

The observed high-lying $\Delta I=1$ level sequence shows some interesting features which can be summarized as follow: (i) The sequence starts at the (11^-) level at 2617.3 keV. The large energy separation to the ground state and other low-lying states indicates a predominantly 4qp nature. (ii) The decay out happens mainly at the (11^-) bandhead state to several low-lying states with positive and negative parity. There is no obvious preference for either parity, pointing also to a 4qp nature of the bandhead. (iii) The band does not show any signature splitting.

The occurrence of enhanced magnetic dipole transitions in the mass $A \approx 200$ has been interpreted in the framework of the tilted-axis cranking model [13,14]. The structure of the so-called ''Shears bands'' is due to a recoupling of the angular momenta of a few nucleons in high-j orbitals at small oblate deformation. So far, these bands have been identified in transitional nuclei at mass number higher than 100. Typical features of such bands are (i) large $M1$ transition probabilities or large $B(M1)/B(E2)$ ratios at the beginning of the band which fall smoothly off with increasing spin and (ii) no signature splitting. The latter effect has been clearly identified from the experimental energies in ^{82}Rb.

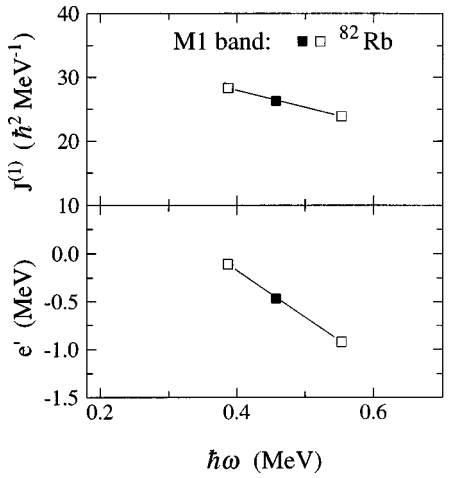

FIG. 10. Kinematic moments of inertia (top) and experimental Routhian (bottom) for the high-lying $M1$ band built on the (11^-) state in ^{82}Rb. Solid (open) symbols have been used for the proposed even-spin (odd-spin) $\Delta I=2$ sequence. A value of $K=6$ has been used in the analysis.

On the other hand, the occurrence of enhanced high-spin $M1$ transitions in the mass 80 region has been previously observed in several odd-mass nuclei, such as the odd-neutron nucleus ^{81}Kr [11] and the odd-proton nuclei ^{81,83,85}Rb [45,46]. It has been demonstrated by shell-model calculations that for odd-proton nuclei with even-N, like ^{85}Rb which is situated in the vicinity of the neutron shell closure at $N=50$, fast $M1$ transitions can also be generated by the 3qp configuration $\pi g_{9/2} \otimes \nu g_{9/2} \otimes \nu f_{5/2}$ [46].

Even though rotation may not play a significant role for the low-lying negative-parity states, the occurrence of the high-lying $M1$ band may point to an onset of a small quadrupole deformation. Therefore, the band has been analyzed using the standard cranked-shell model formalism [36] and the resulting kinematic moments of inertia and the experimental Routhians are shown in Fig. 10 as a function of the rotational frequency. In general, the moments of inertia are somewhat higher, about 20%, when compared with the positive-parity band in ^{82}Rb, and there is no signature splitting at all. The few points available from both signatures follow a straight line.

Assuming a small deformation of ^{82}Rb and negative parity for the $\Delta I=1$ sequence, we suggest the following interpretation: In order to generate a 4qp state of negative parity, an additional nucleon pair has to be broken. If we assume that a proton pair breaks up then the $p_{1/2}$, $p_{3/2}$, $f_{5/2}$, or $g_{9/2}$ subshells can be occupied at proton number $Z=37$. A negative-parity cluster can than be formed by elevation of one unpaired particle into the $g_{9/2}$ subshell. The newly unpaired quasiprotons cannot, however, occupy all the possible

orbitals because of the Pauli principle. The lowest-energy $g_{9/2}$ orbital is already filled by an unpaired quasiproton. Therefore, the quasiprotons can couple at most to a cluster of $(p_{3/2},g_{9/2})$ or $(f_{5/2},g_{9/2})$ with spins of 5^- or 6^-, respectively. This cluster may couple further to the 2qp configuration $(\pi g_{9/2}\otimes\nu g_{9/2})_{6^+,7^+,8^+,9^+}$ to form 4qp states within the spin range $11^-,\ldots,15^-$. Due to the Pauli blocking of the lowest $g_{9/2}$ quasiproton orbital, more excitation energy is needed to generate high-spin states.

It should be noted that essentially the same arguments can be made for two-quasineutron excitations; however, at neutron number 45 the break up of a $p_{3/2}$ or $f_{5/2}$ neutron pair and elevation of one neutron into the $g_{9/2}$ subshell costs much more energy than for a proton pair. Thus, the break of a neutron pair is very unlikely and we propose the 4qp configuration $\pi(g_{9/2})^2\otimes\pi(p_{3/2},f_{5/2})\otimes\nu g_{9/2}$ for the 11^- bandhead state of the new $M1$ sequence.

A rough estimate of the excitation energy of the 11^- state can be made from the sum of the excitation energies of its constituents, namely the 5^- and 6^+ states. The energy needed to form the two-quasiproton 5^- configuration can be deduced from the excitation energies of the lowest 5^- states in adjacent even-even nuclei which have been interpreted as two-quasiproton excitations; e.g., at 2860 keV in ^{80}Kr [47] and 2817 keV in ^{82}Sr [48]. Further, the energies of the 5^- states at 2828 keV in ^{82}Kr [49] and at 2769 keV in ^{84}Sr [50] are similar, resulting in an average energy of 2818 keV. This value has to be added to the 6^+ energy of 191.3 keV yielding about 3 MeV for the 11^- state, which is only 15% larger than the experimental value of 2.6 MeV.

As already mentioned, high-lying $M1$ bands of negative parity were observed in several neighboring odd-mass nuclei, including ^{79}Kr, ^{81,83}Rb, and ^{83}Y. A comprehensive compilation is given in Ref. [12]. It has been suggested that these bands are mainly based on a high-K 3qp configuration involving the $(\pi g_{9/2}\otimes\nu g_{9/2})$ cluster coupled to a negative-parity $(p_{3/2},f_{5/2})$ proton (neutron) for odd-neutron (odd-proton) nuclei. The proposed 4qp configuration for the high-lying 11^- bandhead state in ^{82}Rb is similar in nature.

V. SUMMARY

High-spin states in the odd-odd nucleus ^{82}Rb were studied using the ^{68}Zn(^{18}O,$p3n$) reaction at 56 MeV. The positive-parity sequence was extended up to a $14^{(+)}$ state. Signature inversion has been seen around spin 11, somewhat shifted to higher spins when compared with the lighter odd-odd ^{76,78,80}Rb isotopes. This shift could be a consequence of the expected decrease in quadrupole deformation for increasing N in odd-odd Rb isotopes.

No well-developed rotational bands of negative parity were observed at low-spins. Instead, a high-lying $\Delta I=1$ sequence was found for the first time in an odd-odd nucleus of the mass 80 region. The (11^-) bandhead state at 2617.3 keV is interpreted as a 4qp $\pi(g_{9/2})^2\otimes\pi(p_{3/2},f_{5/2})\otimes\nu g_{9/2}$ state. At a neutron number of 45, when the intruder $g_{9/2}$ subshell is half filled in ^{82}Rb, the competition between the deformation driving $g_{9/2}$ valence proton excitations and the almost spherical $g_{9/2}$ valence neutron excitations results in a lower deformation compared to the neutron-deficient Rb isotopes but still with a rotationlike positive-parity yrast band above spin 8 and a collective high-lying magnetic dipole band.

ACKNOWLEDGMENTS

The authors thank J. X. Saladin for the loan of the Pittsburgh Ge detectors and electronics for the joint Pittsburgh-Florida State Universities detector array. We are grateful to T. D. Johnson for his participation in the early stage of this project and to R. Wyss and W. Nazarewicz for providing the TRS computer codes. Fruitful discussions with H. Schnare and R. Schwengner are acknowledged. This work was supported in part by the National Science Foundation under Grant Nos. PHY-92-10082 with Florida State University and PHY-94-02761 with University of Notre Dame.

[1] J. W. Holcomb, T. D. Johnson, P. C. Womble, P. D. Cottle, S. L. Tabor, F. E. Durham, and S. G. Buccino, Phys. Rev. C **43**, 470 (1991).

[2] J. Döring, J. W. Holcomb, T. D. Johnson, M. A. Riley, S. L. Tabor, P. C. Womble, and G. Winter, Phys. Rev. C **47**, 2560 (1993).

[3] Q. Pan, M. de Poli, E. Farnea, C. Fahlander, D. de Acuña, G. de Angelis, D. Bazzacco, F. Brandolini, A. Buscemi, P. J. Dagnall, A. Gadea, S. Lunardi, D. R. Napoli, C. M. Petrache, M. N. Rao, C. Rossi Alvarez, A. G. Smith, P. Spolaore, G. Vedovato, C. A. Ur, and L. H. Zhu, Nucl. Phys. **A627**, 334 (1997).

[4] A. Harder, M. K. Kabadiyski, K. P. Lieb, D. Rudolph, C. J. Gross, R. A. Cunningham, F. Hannachi, J. Simpson, D. D. Warner, H. A. Roth, Ö. Skeppstedt, W. Gelletly, and B. J. Varley, Phys. Rev. C **51**, 2932 (1995).

[5] R. A. Kaye, J. Döring, J. W. Holcomb, G. D. Johns, T. D. Johnson, M. A. Riley, G. N. Sylvan, P. C. Womble, V. A. Wood, S. L. Tabor, and J. X. Saladin, Phys. Rev. C **54**, 1038 (1996).

[6] G. Winter, R. Schwengner, J. Reif, H. Prade, J. Döring, R. Wirowski, N. Nicolay, P. von Brentano, H. Grawe, and R. Schubart, Phys. Rev. C **49**, 2427 (1994).

[7] S. Chattopadhyay, H. C. Jain, S. D. Paul, J. A. Sheikh, and M. L. Jhingan, Phys. Rev. C **49**, 116 (1994); **47**, R1 (1993).

[8] S. L. Tabor, J. Döring, G. D. Johns, R. A. Kaye, G. N. Sylvan, C. J. Gross, Y. A. Akovali, C. Baktash, D. W. Stracener, P. F. Hua, M. Korolija, D. R. LaFosse, D. G. Sarantites, F. E. Durham, I. Y. Lee, A. O. Macchiavelli, W. Rathbun, and A. Vander Molen, Phys. Rev. C **56**, 142 (1997).

[9] J. Döring, G. Winter, L. Funke, B. Cederwall, F. Lidén, A. Johnson, A. Atac, J. Nyberg, G. Sletten, and M. Sugawara, Phys. Rev. C **46**, R2127 (1992).

[10] S. K. Tandel, S. B. Patel, R. K. Bhowmik, A. K. Sinha, S. Muralithar, and N. Madhavan, Phys. Rev. C **56**, R2358 (1997); Nucl. Phys. **A632**, 3 (1998).

[11] L. Funke, F. Dönau, J. Döring, P. Kemnitz, E. Will, G. Winter, L. Hildingsson, A. Johnson, and T. Lindblad, Phys. Lett. **120B**, 301 (1983); Nucl. Phys. **A455**, 206 (1986).

[12] S. L. Tabor and J. Döring, Phys. Scr. **T56**, 175 (1995).
[13] G. Baldsiefen, H. Hübel, W. Korten, D. Mehta, N. Nenoff, B. V. Thirumala Rao, P. Willsau, H. Grawe, J. Heese, H. Kluge, K. H. Maier, R. Schubart, S. Frauendorf, and H. J. Maier, Nucl. Phys. **A574**, 521 (1994).
[14] S. Frauendorf, Nucl. Phys. **A557**, 259c (1993).
[15] S. Frauendorf, Z. Phys. A **358**, 163 (1997).
[16] G. Graeffe, S. Väisälä and J. Heinonen, Nucl. Phys. **A140**, 161 (1970).
[17] M. Behar, A. Filevich, G. Garcia Bermudeze, M. A. J. Mariscotti, and L. Szybisz, Nucl. Phys. **A337**, 253 (1980).
[18] J. Döring, L. Funke, W. Wagner, and G. Winter, Z. Phys. A **339**, 425 (1991).
[19] J. Döring, L. Funke, G. Winter, F. Lidén, B. Cederwall, A. Johnson, R. Wyss, J. Nyberg, and G. Sletten, in *Proceedings of the International Conference on High Spin Physics and Gamma-Soft Nuclei*, Pittsburgh, 1990, edited by J. X. Saladin, R. A. Sorensen, and C. M. Vincent (World Scientific, Singapore, 1991), p. 381.
[20] J. Döring, D. Ulrich, G. D. Johns, T. D. Johnson, M. A. Riley, and S. L. Tabor, Bull. Am. Phys. Soc. **39**, 1393 (1994).
[21] S. L. Tabor, M. A. Riley, J. Döring, P. D. Cottle, R. Books, T. Glasmacher, J. W. Holcomb, J. Hutchins, G. D. Johns, T. D. Johnson, T. Petters, O. Tekyi-Mensah, P. C. Womble, L. Wright, and J. X. Saladin, Nucl. Instrum. Methods Phys. Res. B **79**, 821 (1993).
[22] W. Gast, K. Dey, A. Gelberg, U. Kaup, F. Paar, R. Richter, K. O. Zell, and P. von Brentano, Phys. Rev. C **22**, 469 (1980).
[23] K. S. Krane, R. M. Steffen, and R. M. Wheeler, Nucl. Data Tables **11**, 351 (1973).
[24] A. Krämer-Flecken, T. Morek, R. M. Lieder, W. Gast, G. Hebbinghaus, H. M. Jäger, and W. Urban, Nucl. Instrum. Methods Phys. Res. A **275**, 333 (1989).
[25] M. Ionescu-Bujor, A. Iordachescu, E. A. Ivanov, and D. Plostinaru, Z. Phys. A **355**, 347 (1996).
[26] P. M. Endt, At. Data Nucl. Data Tables **23**, 547 (1979).
[27] P. C. Womble, J. Döring, T. Glasmacher, J. W. Holcomb, G. D. Johns, T. D. Johnson, T. J. Petters, M. A. Riley, V. A. Wood, and S. L. Tabor, Phys. Rev. C **47**, 2546 (1993).
[28] I. Hamamoto, Phys. Lett. B **235**, 221 (1990).
[29] A. Ikeda and T. Shimano, Phys. Rev. Lett. **63**, 139 (1989).
[30] M. Matsuzaki, Phys. Lett. B **269**, 23 (1991).
[31] A. K. Jain and A. Goel, Phys. Lett. B **277**, 233 (1992).
[32] B. Cederwall, F. Lidén, A. Johnson, L. Hildingsson, R. Wyss, B. Fant, S. Juutinen, P. Ahonen, S. Mitarai, J. Mukai, J. Nyberg, I. Ragnarsson, and P. B. Semmes, Nucl. Phys. **A542**, 454 (1992).
[33] Y. Liu, J. Lu, Y. Ma, S. Zhou, and H. Zheng, Phys. Rev. C **54**, 719 (1996).
[34] J. F. Smith, C. J. Chiara, D. B. Fossan, G. R. Gluckman, G. J. Lane, J. M. Sears, I. Thorslund, H. Amro, C. N. Davids, R. V. F. Janssens, D. Seweryniak, I. M. Hibbert, R. Wadsworth, I. Y. Lee, and A. O. Macchiavelli, Phys. Lett. B **406**, 7 (1997).
[35] A. J. Kreiner and M. A. J. Mariscotti, Phys. Rev. Lett. **43**, 1150 (1979).
[36] R. Bengtsson, S. Frauendorf, and F.-R. May, At. Data Nucl. Data Tables **35**, 15 (1986).
[37] A. Bohr and B. R. Mottelson, *Nuclear Structure* (Benjamin, Reading, MA, 1975), Vol. II, p. 665.
[38] D. J. Hartley, M. A. Riley, D. E. Archer, T. B. Brown, J. Döring, R. A. Kaye, F. G. Kondev, T. Petters, J. Pfohl, R. K. Sheline, and S. L. Tabor, Phys. Rev. C **57**, 2944 (1998).
[39] W. Nazarewicz, J. Dudek, R. Bengtsson, T. Bengtsson, and I. Ragnarsson, Nucl. Phys. **A435**, 397 (1985).
[40] R. Wyss, F. Lidén, J. Nyberg, A. Johnson, D. J. G. Love, A. H. Nelson, D. W. Banes, J. Simpson, A. Kirwan, and R. Bengtsson, Nucl. Phys. **A503**, 244 (1989).
[41] J. C. Hubbs, W. A. Nierenberg, H. A. Shugart, H. B. Silsbee, and R. J. Sunderland, Phys. Rev. **107**, 723 (1957).
[42] C. Thibault, F. Touchard, S. Büttgenbach, R. Klapisch, M. de Saint Simon, H. T. Duong, P. Jacquinot, P. Juncar, S. Liberman, P. Pillet, J. Pinard, J. L. Vialle, A. Pesnelle, and G. Huber, Phys. Rev. C **23**, 2720 (1981).
[43] M. B. White, E. Lipworth, and S. Alpert, Phys. Rev. **136**, B584 (1964).
[44] J. Döring, G. Winter, W. D. Fromm, L. Funke, P. Kemnitz, and E. Will, Z. Phys. A **316**, 75 (1984).
[45] J. Döring, R. Schwengner, L. Funke, H. Rotter, G. Winter, B. Cederwall, F. Lidén, A. Johnson, A. Atac, J. Nyberg, and G. Sletten, Phys. Rev. C **50**, 1845 (1994).
[46] R. Schwengner, G. Winter, J. Reif, H. Prade, L. Käubler, R. Wirowski, N. Nicolay, S. Albers, S. Eßer, P. von Brentano, and W. Andrejtscheff, Nucl. Phys. **A584**, 159 (1995).
[47] J. Döring, V. A. Wood, J. W. Holcomb, G. D. Johns, T. D. Johnson, M. A. Riley, G. N. Sylvan, P. C. Womble, and S. L. Tabor, Phys. Rev. C **52**, 76 (1995).
[48] S. L. Tabor, J. Döring, J. W. Holcomb, G. D. Johns, T. D. Johnson, T. J. Petters, M. A. Riley, and P. C. Womble, Phys. Rev. C **49**, 730 (1994).
[49] P. Kemnitz, P. Ojeda, J. Döring, L. Funke, L. K. Kostov, H. Rotter, E. Will, and G. Winter, Nucl. Phys. **A425**, 493 (1984).
[50] A. Dewald, U. Kaup, W. Gast, A. Gelberg, H.-W. Schuh, K. O. Zell, and P. von Brentano, Phys. Rev. C **25**, 226 (1982).